_____

Pyridazinium-based ionic liquids as corrosion inhibitors for copper in phosphoric acid containing chloride: electrochemical, surface and quantum chemical comparatives studies

A. Bousskri[1], R. Salghi[1],*, A. Anejjar[1], S. Jodeh[2], M. A. Quraishi[3], M. Larouj[4], H. Lgaz[1,4], M. Messali[5], S. Samhan[6] and M. Zougagh[7,8]

[1]*Laboratory of Applied Chemistry and Environment, ENSA, University Ibn Zohr, Agadir, Morocco*
[2]*Chemistry Department, Faculty of Science, Taibah University, Al-Madinah Al-Mounawwara, Saudi Arabia*
[3]*Department of Applied Chemistry, Indian Institute of Technology, Banaras Hindu University, Varanasi-221005, Uttar Pradesh, India*
[4]*Laboratory separation processes, Faculty of Science, University Ibn Tofail, Kenitra, Morocco*
[5]*Chemistry Department, Faculty of Science, Taibah University, Al-Madinah Al-Mounawwara, Saudi Arabia*
[6]*Palestine Water Authority, Ramallah, Palestine*
[7]*Regional Institute for Applied Chemistry Research, IRICA, E-13004, Ciudad Real, Spain*
[8]*Castilla-La Mancha Science and Technology Park, E-02006, Albacete, Spain*
_____

ABSTRACT

*The acid corrosion inhibition and adsorption process of copper in 2M H3PO4 containing 0.3M of NaCl by an Eco-friendly ionic liquid newly synthesized [1-(2-(4-chlorophenyl)-2 oxoethyl)Pyridazinium Bromid **CPEPB**] and [1-(2-(4-nitrophenyl)-2-oxoethyl)Pyridazinium Bromide **NPEPB**]. Was studied by using weight loss measurements, electrochemical impedance spectroscopy (EIS) and potentiodynamic polarization.The presence of these tow molecules led to decrease of the corrosion rate of Copper. At 10^{-3} M of **NPEPB** and **CPEPB,** the inhibition efficiencies increase with the inhibitor concentration to reach 88.94% and 87.5%, respectively. The adsorption of these compounds on Copper surface agrees Langmuir's adsorption isotherm. To support the experimental results and To perform the corrosion study, Quantum chemical approach, using the density functional theory (DFT), was applied in order to get better understanding about the relationship between the inhibition efficiency and molecular structure of **NPEPB** and **CPEPB**. The parameters include the lowest unoccupied molecular orbital (LUMO), highest occupied molecular orbital (HOMO), amount of electrons transferred and dipole moment. The results of the study suggest that **NPEPB** is a better corrosion inhibitor than **CPEPB**, which is in agreement with most experimental results obtained at different concentrations.*

Keywords: Corrosion inhibition; phosphoric acid; Adsorption; Copper; Pyridazinium-based ionic liquid.
_____

INTRODUCTION

Due to the large aggressive acidic solutions, Inhibitors are frequently used to reduce the corrosive attack on metallic materials. The use of inhibitors is one of the most sensible methods for the protection of metals against corrosion especially in phosphoric acid environment [1,2]. Phosphoric acid is largely used in industries, for example, acid pickling, in the food industry, acid desalting and acid cleaning. Copper is a metal widely used in industry, because of his mechanical properties and a good thermal conductivity. However, it readily reacts in environments containing ordinary oxygen. Thus, the study of its corrosion inhibition has attracted much attention. Most work on copper corrosion reveals that the presence of aggressive elements such as chloride and sulfide accelerates the corrosion of this metal [3–5]. The use of inhibitors is one of the most practical methods for protection against corrosion,

_____

especially in acidic media [6]. There are various organic inhibitors which tend to decrease the corrosion rate of copper in acidic solutions [7–11]. Electronegative functional groups and π-electron in triple or conjugated double bonds as well as heteroatom like sulphur, phosphorus, nitrogen and oxygen in their structures are the major adsorption centers. Recently the research has been focused on the use of the Eco-friendly products or green inhibitors are known to have inhibitive action [12, 13 –16]. In the last two decades, the organic compounds with low melting points which known as Ionics liquids (ILs), were considered as important topic of research in both industry and academia [17]. There are also wid ange of applications of these Ionics liquids [18-22]. The inhibitors that can be reducing corrosion on metallic materials can be divided in to three kinds: (a) organic inhibitors, (b) inorganic inhibitors and (c) mixed material inhibitors [23]. The inhibitory effect of Pyridazinium-based Ionic Liquid [24], azoles [25-33], and some ionic liquids derivatives such as imidazolium [34] is studied. Recently, Ionic liquids have been also widely investigated for a variety of applications [35–38], they showed very survey properties such as inflammability, thermal stability, moderate solubility for inorganic and organic compounds, electrochemical potential properties and high ionic conductivity [39-43]. It's reported that, both pyridinium and imidazolium compounds are reported to represent a good corrosion inhibitors on copper [44, 45], steel [46-49] and aluminium [50]. The aim of the these study was to assess comparatively the inhibition effect of two ionic liquids namely [1-(2-(4-chlorophenyl)-2 oxoethyl) Pyridazinium Bromide *CPEPB*] and [1-(2-(4-nitrophenyl)-2-oxoethyl) Pyridazinium Bromide *NPEPB*] on Copper in 2M H_3PO_4 solution containing 0.3M NaCl using gravimetric measurements, polarization measurements, electrochemical impedance spectroscopy, quantum chemical calculations and Optical microscopy (OM), for the surface morphology. The compound's chemical structures are given in Table1.

MATERIALS AND METHODS

2.1. Materials
The working electrode used in this work is a copper with a chemical composition (in wt%) of 0.01 % Ni, 0.019 % Al, 0.004 % Mn, 0.116 % Si and **99.5** % Cu Prolabo Chemicals. Prior to all measurements, the copper samples were pre-treated by grinding with emery paper SiC (180, 600, 1200 and 2000); rinsed with distilled water, degreased in ethanol in an ultrasonic bath immersion for 5 min, washed again with bidistilled water and then dried at room temperature before use.

2.2. Chemical Compound
The organic compound tested was structure [1-(2-(4-chlorophenyl)-2 oxoethyl) Pyridazinium Bromide **CPEPB**] and [1-(2-(4-nitrophenyl)-2-oxoethyl) Pyridazinium Bromide **NPEPB**]. There was synthesized as described elsewhere [35] **(Table1).**

Table1. The chemical structure of the studied Pyridazinium-based ionic liquids

Abbreviation	Structural Formula	Name
CPEPB		**1-(2-(4-chlorophenyl)-2-oxoethyl) Pyridazinium Bromide**
NPEPB		**1-(2-(4-nitrophenyl)-2-oxoethyl) Pyridazinium Bromide**
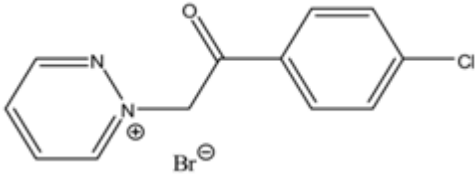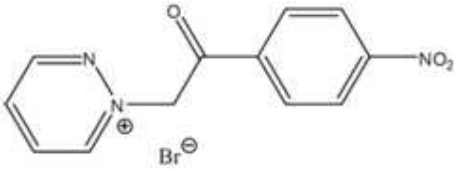
2.3. Solutions
The experiments were carried out in 2M H_3PO_4 medium containing 0.3M of NaCl. The solution tests are freshly prepared before each experiment; it was prepared by dilution of Analytical Grade 85% H_3PO_4 with bidistilled water and pure NaCl. The ionic liquids tested were [1-(2-(4-chlorophenyl)-2 oxoethyl) Pyridazinium Bromide **CPEPB**] and [1-(2-(4-nitrophenyl)-2-oxoethyl) Pyridazinium Bromide **NPEPB**].The concentration range of these compounds was 10^{-3} to 10^{-6} M.

_____

2.4. Weight loss measurements

Gravimetric methods were conducted on copper and carried out at definite time interval of 8 h at room temperature using an analytical balance (precision $\pm$ 0.1 mg). All experiments were carried out under total immersion in 80 ml of test solutions. The copper specimens used of a total surface of 12 cm2. Prior to each gravimetric or electrochemical experiment, the exposed area was mechanically abraded with 180, 320, 800, 1200 grades of emery papers, rinsed thoroughly with acetone and bidistilled water before plunging the electrode in the solution. Pure copper samples (99.5%) were used. The experiments were carried out in 2 M H_3PO_4 medium containing 0.3M of NaCl, it was prepared by dilution of Analytical Grade 85% H_3PO_4 with bidistilled water and pure NaCl.

2.5. Polarization measurements

2.5.1. Electrochemical impedance spectroscopy (EIS)

The electrochemical measurements were performed by using Voltalab (Tacussel-Radiometer PGZ 100) potentiostat and controlled by Tacussel corrosion analysis software model (Voltamaster 4) under static condition. The cell of corrosion used had three electrodes. The reference electrode was a saturated calomel electrode (SCE). An electrode of platinum was used as auxiliary electrode. The working electrode was carbon steel. All the potentials given in our study were referred to this reference electrode. The working electrode was immersed in test solution for 30 minutes to establish a steady state open circuit potential (E_{ocp}). After measuring the Eocp, the electrochemical measurements were carried out. All electrochemical tests were carried out in aerated solutions at 298 K. The response of the electrochemical system to ac excitation with a frequency ranging from 10^5 Hz to 10^{-1} Hz and peak to peak amplitude of 10 mV was measured with data density of 10 points per decade. Nyquist diagrams were made starting from these experiments. The best semicircle can be fit through the data points in the Nyquist diagram using a non-linear least square fit so as to give the intersections with the **x**-axis.

2.5.2. Polarization curves

The electrochemical behaviour of the electrod of cooper in inhibited and uninhibited solution was studied by recording cathodic and anodic potentiodynamic polarization curves. Measurements were carried out in the 2M H_3PO_4 medium containing 0.3M of NaCl solution containing different concentrations of the inhibitor, after 30 min of immersion, by changing the electrode potential automatically from -600 mV to 100 mV versus corrosion potential at a scan rate of 1 mV.s^{-1}. The corrosion current densities (I_{corr}) were obtained by extrapolation of linear Tafel segments of anodic and cathodic curves to corrosion potential (E_{corr}).

2.6. Optical microscopy measurements (OM)

Immersion corrosion analysis of Copper sample in the acidic solutions with and without the optimal concentration of the tow inhibitors *NPEPB* and *CPEPB* was performed using Optical microscopy 6 h at 298K respectively. After the corrosion tests, the samples were immediately subjected to OM studies to find the morphological changes on copper. **(OM Best.Scope)** was used for the experiments. The working sample was analyzed at three different locations to ensure reproducibility.

2.7. Quantum Chemical Calculations

Full geometry optimization with no constraints of **NPEPB** and **CPEPB** were performed using DFT based on Beck's three parameter exchange functional and Lee–Yang–Parr nonlocal correlation functional (B3LYP) [51-53] and the 6-31g(d,p) orbital basis sets for all atoms as implemented in Gaussian 03 program [54]. The calculated molecular properties include the highest occupied molecular orbital (HOMO), lowest unoccupied molecular orbital (LUMO) and other molecular properties derived from HOMO and LUMO and their respective energies. Molecular modeling study was carried out to determine the electron rich groups/atoms in a molecule as well as calculation of the highest molecular orbital (HOMO) and lowest unoccupied molecular orbital (LUMO) in order to give further insights on the possibility of electron transfer between the inhibitor and metal.

RESULTS AND DISCUSSION

3.1.Potentiodynamic polarization curves

The effect of **NPEPB** and **CPEPB** on the corrosion reactions was determined by polarization techniques. The changes observed in the polarization curves after the addition of the inhibitor are usually used as the criteria to classify inhibitors as cathodic, anodic or mixed type [55, 56].
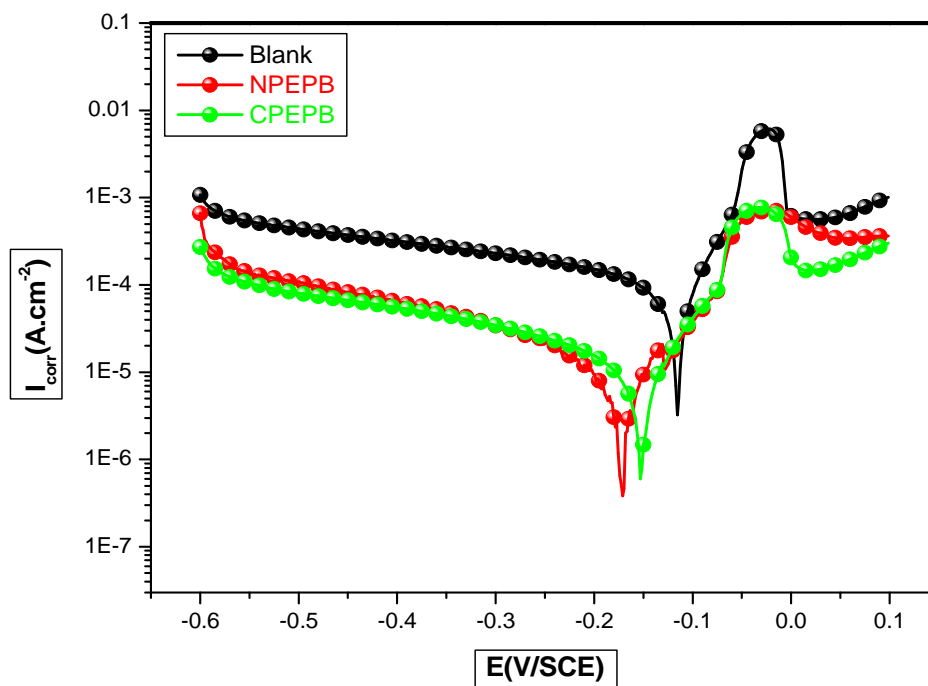
Fig 1. Potentiodynamic polarization curves of Copper in (2M H$_3$PO$_4$ + 0.3M NaCl) in absence and presence of optimum concentration of NPEPB and CPEPB at 298 K

Fig.1 shows the Tafel polarization curves for Copper in 2M H$_3$PO$_4$ medium containing 0.3M of NaCl at optimum concentration 10^{-3} M of inhibitors at 298 K. The potentiodynamic parameters (Table2) such as corrosion potential (E$_{corr}$), cathodic Tafel slopes (b$_c$), corrosion current density (I$_{corr}$), were obtained from Tafel plots and the inhibition efficiency values E$_I$ (%), were calculated using equation1.

$$E_I \ \% \ = \ \frac{I_{corr} - I'_{corr}}{I_{corr}} \ \times 100 \tag{1}$$

Where I$_{corr}$ and I'$_{corr}$ are uninhibited and inhibited corrosion current densities, respectively.

Under the experimental conditions performed, the cathodic branch represents the hydrogen evolution reaction, while the anodic branch represents the iron dissolution reaction. These branches are determined by extrapolation of Tafel lines to the respective corrosion potentials.

Analysis of the polarization curves indicates that the inhibitor **NPEPB** and **CPEPB** studied leads both to decrease the cathodic and anodic current densities and decrease in the corrosion rate. There was no remarkable shift in the corrosion potential (E$_{corr}$) value with respect to the blank. Indeed according to literature report [57], when corrosion potential is more than ±85 mV with respect to the corrosion potential of the blank, the inhibitor can be considered distinctively as either cathodic or anodic type. However, the maximum displacement in this study is less than ±85 mV. As can be seen from Table 2, E$_{corr}$ values did not change significantly (only the displacement was < 56 mV) in presence of inhibitors, based on the marked decrease of the cathodic and anodic current densities upon introducing the inhibitor in the aggressive solution, **NPEPB** and **CPEPB** can be considered as a mixed-type inhibitors but favoring the cathodic side more, and also meaning that the addition of the inhibitors reduces the anodic dissolution and also retards the cathodic hydrogen evolution reaction.

_____

Table 2. Electrochemical parameters of copper at various concentrations of NPEPB and CPEPB in (2M H₃PO₄+ 0.3M NaCl) and the corresponding inhibition efficiency

Inhibitors	Conc. (M)	-E$_{corr}$ (mV/SCE)	I$_{corr}$ (µA/cm²)	-b$_c$ (mV/dec)	E$_{Tafel}$ (%)
	Blank	**118**	**149**	**322**	**-**
CPEPB	**10⁻³**	154	19	253	**87.25**
	10⁻⁴	137	30	320	79.87
	10⁻⁵	155	40	280	73.15
	10⁻⁶	157	85	250	42.95
NPEPB	**10⁻³**	174	18	253	**88.00**
	10⁻⁴	182	24	253	83.89
	10⁻⁵	156	57	220	61.74
	10⁻⁶	156	100	210	32.89

All the electrochemical parameters deduced from **Fig1** are summarized in **Table 2**, inspecting the results We note that the corrosion current density I$_{corr}$ decreases monotonically when the content of **NPEPB** and **CPEPB** increases in solution, and the maximum percentage of inhibition efficiency (**E$_{Tafel}$ (%)**) was achieved at the low concentration of 10⁻³M reaching 88% for **NPEPB** and 87.25% for **CPEPB.** The classification of these inhibitors according to their inhibition efficiency is:

<div align="center">

NPEPB > CPEPB

</div>

3.2. Electrochemical Impedance Spectroscopy Measurements EIS

The corrosion behavior of Copper in the aggressive medium (2M H₃PO₄ + 0.3M NaCl) solution in the presence of NPEPB and CPEPB, was investigated by (EIS) at room temperature after 30 min of immersion at E$_{corr}$. Nyquist plots in absence and presence of optimum concentration 10⁻³M of inhibitors (NPEPB and CPEPB) are given in Fig.2 and their corresponding parameters were calculated by using Nyquist plots are given in Table 3. At open circuit, the spectrum shows one capacitive loop. In the presence of NPEPB and CPEPB, the capacitive loop size increases. The charge-transfer resistance (R$_{ct}$) values are calculated from the difference in impedance at lower and higher frequencies, as suggested by Tsuru et al [58]. The double layer capacitance (C$_{dl}$) and the frequency at which the imaginary component of the impedance is maximal (-Z$_{max}$) are found as represented in equation 8:

$$C_{dl} = \frac{1}{\omega R_{ct}} \qquad \text{Where} \qquad \omega = 2\pi f_{max} \qquad\qquad (2)$$

As observed, the Nyquist plots contain a depressed semi-circle with the center below the real X-axis, which is size increased by increasing the inhibitor concentrations, indicating that the corrosion of copper is mainly a charge transfer process [59] and the formed inhibitive film was strengthened by the increasing the concentration of the two inhibitors.
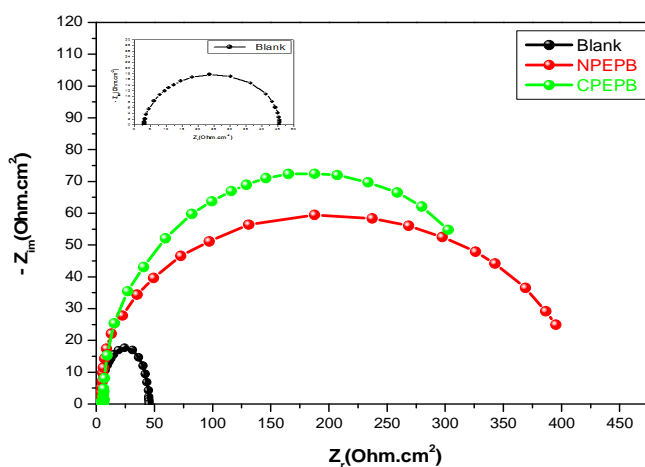
Fig 2: Nyquist diagrams for copper electrode in (2M H₃PO₄+ 0.3M NaCl) in absence and presence of optimum concentration *10⁻³M* of inhibitors (*NPEPB* and *CPEPB*)

_____

The quantitative analysis of the electrochemical impedance spectra (EIS) was studied based on a physical model of the corrosion process with hydrogen depolarization and with charge transfer controlling step. The simplest model includes the charge transfer resistance (R_{ct}) in parallel to the capacitance (C_{dl}) connected with the solution resistance (Rs). The equivalent circuit model employed for this system is presented in Fig.3.
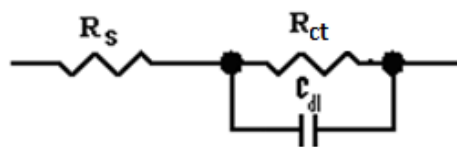
Fig. 3 The electrochemical equivalent circuit used to fit the impedance spectra

The obtained impedance diagrams are almost in a semi-circular appearance, indicating that the charge - transfer process mainly controls the corrosion of Copper. Deviations of perfect circular shape are often referred to the frequency dispersion of interfacial impedance. This anomalous phenomenon may be attributed to the inhomogeneity of the electrode surface arising from surface roughness or interfacial phenomena. In fact, in the presence of the MS195 (PPB), the value of Rct has enhanced and the values of double layer capacitance are also brought down to the maximum extent. The decrease in C_{dl} shows that the adsorption of the inhibitors takes place on the metal surface in acidic solution. The impedance parameters derived from these plots are shown in Table 3.

Table 3. Electrochemical Impedance for corrosion of copper in acid medium at various concentrations of NPEPB and CPEPB

Inhibitors	Conc. (M)	Rct ($\Omega.cm^2$)	$C_{dl}(\mu F/cm^2)$	E_{Rct} (%)
	Blank	45	354	-
	10^{-3}	360	6	87.5
	10^{-4}	240	16	81.25
CPEPB	10^{-5}	172	25	73.84
	10^{-6}	80	70	43.75
	10^{-3}	407	6	88.94
	10^{-4}	287	11	84.32
NPEPB	10^{-5}	120	54	62.5
	10^{-6}	62	135	27.42

Again, the maximum percentage of inhibition efficiency (E_{Rct} %) was achieved at the low concentration of 10^{-3}M reaching 89% for NPEPB and 87.5% for CPEPB. The classification of these inhibitors according to their inhibition efficiency is: NPEPB > CPEPB.

This percent inhibition efficiency is calculated by charge transfer resistance obtained from Nyquist plots, according to the equation 3:

$$E_{Rct} \% = \frac{R'_{ct} - R_{ct}}{R'_{ct}} \times 100 \qquad (3)$$

Where R_{ct} and R'_{ct} are the charge transfer resistance values without and with inhibitor, respectively.

3.3. Weight loss measurements and adsorption isotherm

Weight loss measurement was done according to the method described previously [60]. And is a non-electrochemical technique for the determination of corrosion rates and inhibitor efficiency which provides more reliable results than electrochemical techniques because the experimental conditions are approached in a more realistic manner yet the immersions tests are time-consuming [61-62]. Therefore, due to such differences often due to the experimental conditions, the values would obviously differ from the values of the electrochemical measurements. All the tests were conducted in aerated 2M H_3PO_4 medium containing 0.3M NaCl at 298 K with different concentrations of the tow inhibitors NPEPB and CPEPB. And the Values of the inhibition efficiency and corrosion rate obtained from the weight loss measurements of Copper for different concentrations of new ionic liquids derivatives NPEPB and CPEPB in phosphoric acid medium containing chloride at 298 K after 6h of immersion are given in Table 4. At the end of the tests the specimen were carefully washed in acetone and then weighed. Duplicate experiments were performed in each and the mean value of the weight loss has been reported. The inhibition efficiency (E_w %), the corrosion rate (W_{corr}), and surface coverage (θ) were determined by using the following equations:

_____

$$W_{corr} = \frac{\Delta m}{S.t} \tag{4}$$

$$E_w \% = \frac{W_{corr} - W'_{corr}}{W_{corr}} \times 100 \tag{5}$$

$$\theta = 1 - \frac{W'_{corr}}{W_{corr}} \quad \Rightarrow \quad \theta = \frac{E_w (\%)}{100} \tag{6}$$

where W_{corr} and W'_{corr} are the corrosion rates of Copper due to the dissolution in 2M H_3PO_4 medium containing 0.3M NaCl in the absence and the presence of definite concentration of inhibitor, respectively, and θ is the degree of surface coverage of the inhibitor.

Table 4: Gravimetric results of Copper in phosphoric acid medium. without and with addition of inhibitors at 298 K, The exposure time is 6h

Inhibitors	Conc (M)	W_{corr} (mg. cm^{-2} h^{-1})	E_w (%)	Θ
	Blank	0.162	-	-
	1×10^{-3}	0.0219	86.48	0.864
	1×10^{-4}	0.0327	79.81	0.798
CPEPB	1×10^{-5}	0.0444	72.59	0.725
	1×10^{-6}	0.0925	42.9	0.429
	1×10^{-3}	0.0192	88.15	0.881
	1×10^{-4}	0.0271	83.27	0.833
NPEPB	1×10^{-5}	0.0622	61.6	0.616
	1×10^{-6}	0.112	30.86	0.309

The values of inhibition efficiency E_w (%) for two inhibitors are given in Table 4. This show that the inhibition efficiency increases with the increasing inhibitor concentration Fig3, and Maximum E_w% (88.15%) of NPEPB was achieved at 10^{-3} M. These results reveal that the compounds under investigation NPEPB and CPEPB are fairly efficient inhibitors for copper dissolution in 2M H_3PO_4 medium containing 0.3M NaCl solution. The inhibition of corrosion of Copper by new ionic liquids derivatives can be explained in terms of adsorption on the metal surface. These compounds can be adsorbed on the Copper surface by the interaction between lone pairs of electrons of nitrogen atoms of the inhibitors and the metal surface. In order to understand the mechanism of corrosion inhibition, the adsorption behavior of the adsorbate on the Copper surface must be known. Two main types of interaction can describe the adsorption of the molecule of NPEPB and CPEPB, physisorption and chemisorption. These are influenced by the chemical structure of the inhibitor, the type of the electrolyte and the charge and nature of the metal. Careful inspection of these results showed that, the ranking of the inhibitors according to E_w (%) is as follows: NPEPB > CPEPB for the same concentration. A plot between inhibition efficiency E_w (%) and inhibitors concentration is shown in Fig.4. Analyse of Fig.4 reveals that as the concentration of inhibitors increases inhibition efficiency E_w (%) increases. This is because more surface area of copper is covered by increasing inhibitors concentration.

3.4. Adsorption isotherm and thermodynamic parameters
The information on the interaction between the inhibitors molecules of NPEPB and CPEPB and the metal surface can be provided by adsorption isotherm. The degree of surface coverage (θ) for different concentrations of inhibitors was evaluated from Weight loss measurements. Attempts were made to fit θ values to various isotherms including Frumkin, Temkin and Langmiur. It was found that the data best fit was obtained with the Langmiur isotherm Fig 5. According to this isotherm θ is related to concentration inhibitor [63].

$$\frac{C}{\theta} = \frac{1}{K} + C \tag{7}$$

Where K is the adsorption/desorption equilibrium constant, C is the corrosion inhibitor concentration in the solution

$$\log K = -1,74 - \left(-\frac{\Delta G_{ads}}{2,303\ RT} \right) \tag{8}$$

Where ΔG_{ads} is the free energy of adsorption.

_____
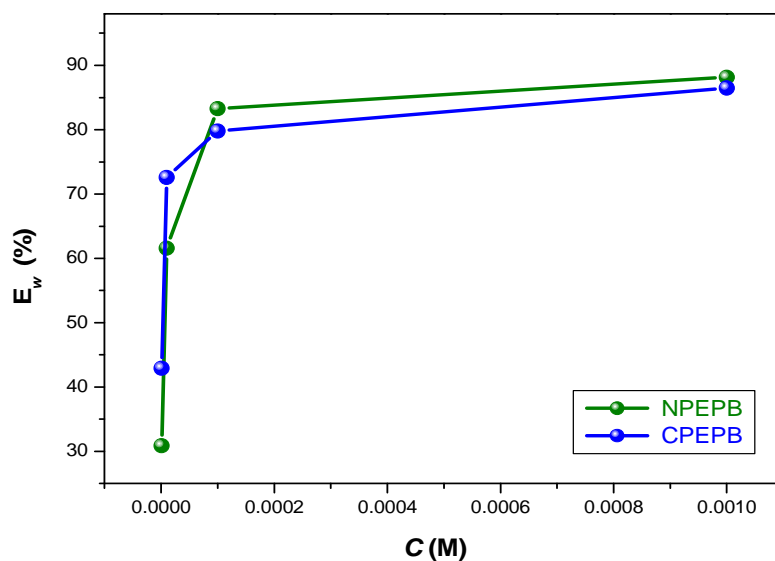
Fig.4. Variation of the inhibition efficiency (Ew %) of Copper corrosion with the concentration of NPEPB and CPEPB in 2M H₃PO₄ + 0.3M NaCl at 298 K
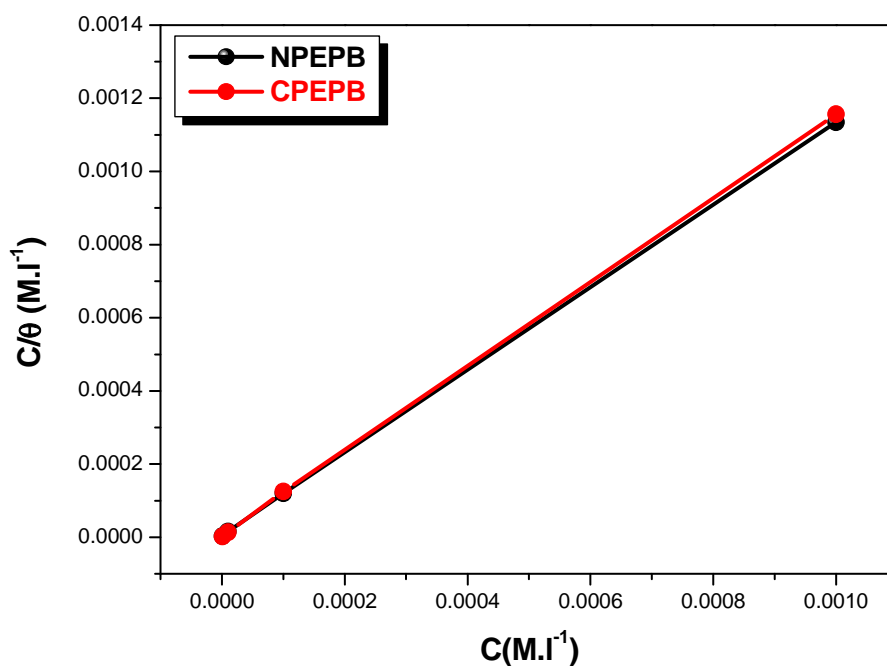
Fig.5: Plots of Langmuir adsorption isotherm in the presence of *NPEPB* and *CPEPB* on the Copper surface at 298K

It was found that Fig.5 (plot of $\dfrac{\theta}{C}$ versus C) gives straight line with slope near to 1, indicating that the adsorption of compound under consideration on Copper/ acidic solution interface obeys Langmiur's adsorption.

_____

Table 5. The thermodynamic parameters for the corrosion of Copper in 2M H₃PO₄ + 0.3M NaCl in the absence and presence of different concentrations of NPEPB and CPEPB

Inhibitors	Slope	K_{ads} (M^{-1})	R^2	ΔG^0_{ads} (kJ/mol)
CPEPB	1.15256	232000	0.999	-40.54
NPEPB	1.13007	463000	0.999	-40.37

The free energy of adsorption (ΔG^0_{ads}) can be calculated from the K_{ads} value obtained from the above correlation:

$$\Delta G_{ads} = -RT \ \ln(55.5 \ x \ K_{ads})$$

(9)

Where 55.5 is the concentration of water, R is the universal gas constant and T is the absolute temperature.

All the obtained thermodynamic parameters are shown in Table 5. The negative values of ΔG^0_{ads} for NPEPB and CPEPB indicate the spontaneous of the adsorption of this inhibitors and stability of the adsorbed layer on the copper surface. More negative value designates that inhibitors are strongly adsorbed on the steel surface. Literature pointed that values of ΔG^0_{ads} around -20 kJ.mo-1 or lower are related to the electrostatic interaction between the charged molecules and the charged metal (physisorption); those around -40 kJ.mol-1or higher involve charge sharing or transfer from organic molecules to the metal surface to form a coordinate type of bond (chemisorption) [64-66].The obtained values of ΔG^0_{ads} surrounded -40 kJ.mol^{-1} indicating, that the adsorption mechanism of the Pyridazinium-based ionic liquids NPEPB and CPEPB tested on copper in 2M H₃PO₄ medium containing chloride solution was of chemical adsorption on the charged Copper surface (Table.5). From (Fig.6). The inhibition efficiencies, calculated for the same concentration from weight loss measurements and electrochemical studies, showed that, the ranking of the inhibitors according to E(%) is as follows: NPEPB > CPEPB.
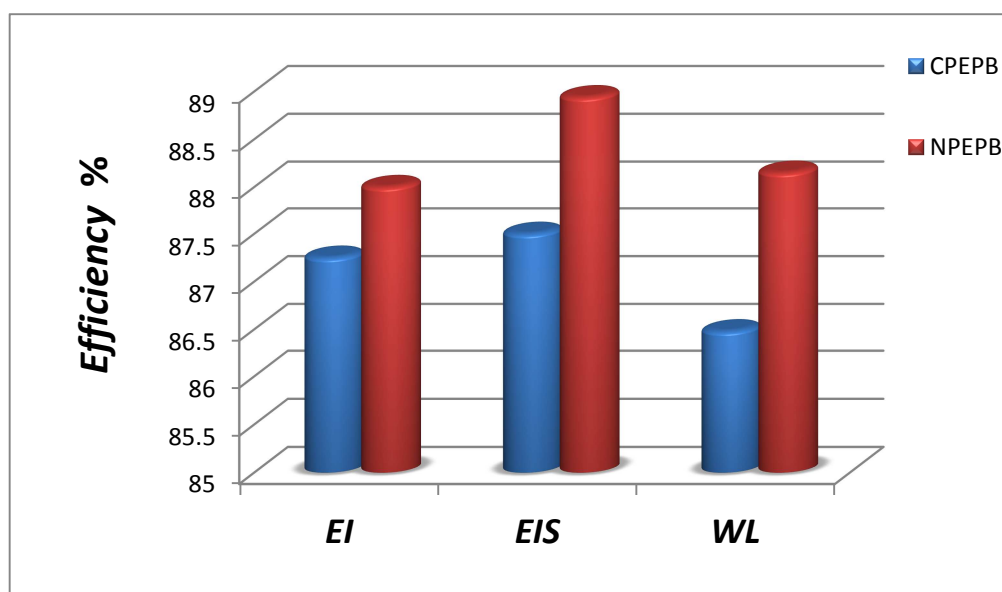
Fig.6: Comparison of inhibition efficiency (E %) values obtained by weight loss, polarization and EIS methods at optimum concentration 10^{-3}M of inhibitors (NPEPB and CPEPB)

3.5. Computational Study

Complete geometrical optimizations of the investigated molecules were performed using DFT (density functional theory) method with the Yang–Parr non local correlation functional (B3LYP) with 6-31 G (d, p) basis set [67-69]. This approach was shown to yield favorable geometries for wide variety of systems and this basis set gives good geometry optimizations. In all cases, total structures optimization together with the vibrational analysis of the optimized structures are implemented by means of Gaussian 03 program package [70] in order to determine whether they correspond to a maximum or a minimum in the potential energy curve and no imaginary frequency was found, indicating minimal energy structures. Frontier molecular orbitals (HOMO and LUMO) could be used to predict the adsorption centers of the inhibitor molecule. For the simplest transfer of electrons, adsorption should occur at the part of the molecule where the softness, σ, which is a local property, has the highest value.

_____

According to Koopman's theorem [71], the E_{HOMO} and E_{LUMO} of the inhibitor molecule are related to the ionization potential, IE, and the electron affinity EA, respectively, by the following relations [10, 11]:

$$IE = -E_{HOMO} \qquad\qquad\qquad\qquad (10)$$

$$EA = -E_{LUMO} \qquad\qquad\qquad\qquad (11)$$

Absolute electro negativity, (χ), and absolute hardness, (η), of the Inhibitor molecules are given by [72]:

$$\chi = \frac{IE + EA}{2} \qquad (12) \qquad\qquad \eta = \frac{IE - EA}{2} \qquad (13)$$

The obtained values of (χ) and (η) are used to calculate the fraction of electron transferred, (ΔN), from the inhibitor to metallic surface as follow [73]:

$$\Delta N = \frac{\chi_{Fe} - \chi_{inh}}{2(\eta_{Fe} + \eta_{inh})} \qquad\qquad (14)$$

Where χ_{Fe} and χ_{inh} denote the absolute electronegativity of iron and inhibitor molecule η_{Fe} and η_{inh} denote the absolute hardness of iron and the inhibitor molecule respectively. In this study, we use the theoretical value of χ_{Fe} =7.0 eV and $\eta_{Fe} = 0$, for calculating the number of electron transferred. The inhibition of copper using substituted pyridazin as corrosion inhibitors were investigated experimentally. The classification of these inhibitors according to its inhibition efficiency is: NPEPB > CPEPB. It was found that the NPEPB molecule among the investigated compounds has the highest inhibition efficiency on the metal surface. The higher inhibition efficiency of NPEPB compound than the other inhibitors is probably due to the high polarizability of C-N bond. Moreover, it is evident to attribute the lower performance of NPEPB to the replacement of –Cl group by –NO$_2$ group. Also, the higher inhibition efficiency of NPEPB is probably referred to the increasing the number of centers of adsorption on the inhibitor molecules and the higher electron densities caused by the electron releasing –NO$_2$ group [74]. Quantum chemical parameters obtained from the calculations which are responsible for the inhibition efficiency of inhibitors, such as the energies of highest occupied molecular orbital (E_{HOMO}), energy of lowest unoccupied molecular orbital (E_{LUMO}), the separation energy (E_{LUMO} - E_{HOMO}), ΔE, representing the function of reactivity, the net charge on the functional group, dipole moment,(μ), total energy (TE), softness (σ) and the fraction of electrons transferred from the inhibitor to copper surface (ΔN), are collected in Table 6. Previous studies confirmed the fact that in aqueous acidic solution the pyridazin molecules get protonated and exist either as neutral molecules or in the form of cations [75]. The pyridazin may adsorb on the metal surface in the form of neutral molecules or in the form of protonated molecules involving the displacement of water molecules from the metal surface and sharing of electrons between the nitrogen atoms in the pyridazin molecule and the metal surface. The other possibility is that the protonated pyridazin molecules may adsorb through electrostatic interaction between positively charged pyridazin molecules and negatively charged metal surface [76-77].

Table.6 The calculated quantum chemical parameters for the neutral inhibitors using DFT/B3LYP/6-31G (d, p)

Molecule	E_{HOMO} (eV)	E_{LUMO} (eV)	ΔE(eV)	μ(eV)	TE(eV)	η(eV)	σ (eV^{-1})	χ(eV)	ΔN	E (%)
NPEPB	-4.0147	-2.8639	1.1507	4.9925	-23212.6	0.5754	1.7379	3.4393	3.094	89
CPEPB	-3.8215	-1.7785	2.0430	3.5171	-30154.1	1.0215	0.9789	2.8000	1.911	87.5

_____
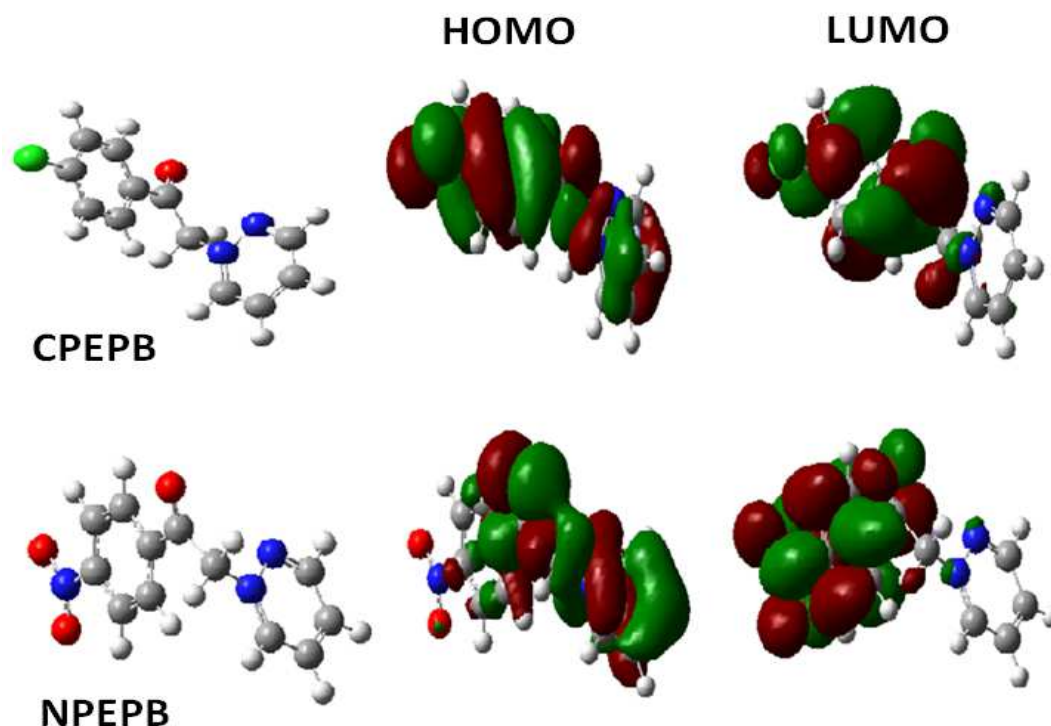
Figure 7: The optimized molecular structures, HOMO and LUMO for the inhibitors using DFT/B3LYP/6-31G (d,p)

The ionization potential (IE) is a quantum parameter connected with the electronic structure which reflects the electron density at the reaction center. The higher the energetic level of (HOMO), the less is the value of the ionization potential; electrons from HOMO are easily donated. Organic substances with less negative HOMO value corresponding lower IE values which are expected to have greater adsorption ability and better inhibition efficiency [78]. It was shown from the calculation that NPEPB which has the highest inhibition efficiency has the highest E_{HOMO}. If the energy of HOMO level was decisive for the inhibitor properties, the ranking of the compounds should be: NPEPB > CPEPB. This agrees well with the experimental observations. Another parameter of the molecular structure is energetic level of (LUMO), which determines the polarizability of the compound i.e. the ability to be distorted by an electric field, and hence LUMO level receives electrons. In this case, the reaction is characterized with transfer of electrons from the metal to the inhibitor. The calculations also show that NPEPB has the lowest E_{LUMO}, so it has the greatest ability to interact with the metal surface. The separation energy, $\Delta E = (E_{LUMO} - E_{HOMO})$ is an important parameter as a function of reactivity of the inhibitor molecule towards the adsorption on metallic surface. As ΔE decreases, the reactivity of the molecule increases leading to increase the inhibition efficiency of the molecule. The results obtained from quantum chemical calculation are listed in Table 6. The calculations indicate that NPEPB has the lowest value which means the highest reactivity among the other inhibitor CPEPB and accordingly the highest inhibition efficiency which agrees well with the experimental observations. The order of reactivity in this case will be: NPEPB > CPEPB. The number of electrons transferred (ΔN) was also calculated depending on the quantum chemical method as in Eq. (1). Values of ΔN showed that the inhibition efficiency resulting from electron donation agreeing with Lukovits's study [79]. If $\Delta N < 3.6$, the inhibition efficiency increases by increasing electron-donating ability to the metal surface and the order by which the ability of these inhibitors to donate electrons to the metal surface increase is: NPEPB > CPEPB. The values of ΔN indicate trends within a set of molecules, but their absolute value might not correspond to reality. ΔN values are not exactly the number of electrons leaving the donor and entering the acceptor molecule. The expression ''electron-donating ability'' is more adequate than ''number of transferred electrons'' [80]. Another quantum chemical parameters such as the dipole moment (μ) is also calculated where the NPEPB compound has the highest value and accordingly the highest inhibition efficiency. The calculations show that we have the same order of reactivity NPEPB > CPEPB. The high values of μ probably mean the increase of the adsorption of inhibitor and accordingly increasing the inhibition efficiency [81-82] which agree with the experimental results. The bonding tendencies of the inhibitors towards the metal atom can be discussed in terms of the HSAB (hard–soft-acid–base) and the frontier-controlled interaction concepts [83-84]. General rule suggested by the principle of HSAB, is that hard acids prefer to co-ordinate to hard bases and soft acids prefer to co-ordinate to soft bases. On the other hand, metal atoms are known as soft acids. Hard molecules have a high HOMO–LUMO gap and soft molecules have a small HOMO–LUMO gap [16], and thus soft bases inhibitors are the most effective for metals. So, the NPEPB compound which has the lowest energy gap and the highest softness has the most be confirmed by calculating another quantum chemical parameter, σ, which

_____

measures the softness of the molecule and so its reactivity: σ = 1/ η, Table 6. It was observed that NPEPB compound has the highest σ value and the order at which softness increase as well as reactivity will be: NPEPB > CPEPB
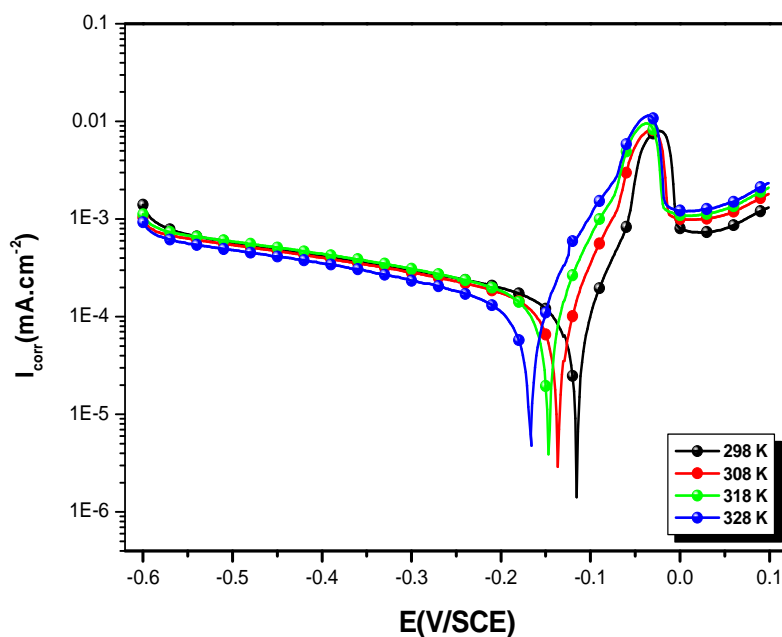
Fig 8 : Potentiodynamic polarization curves of copper in (2M H₃PO₄ + 0.3M NaCl) at different temperatures
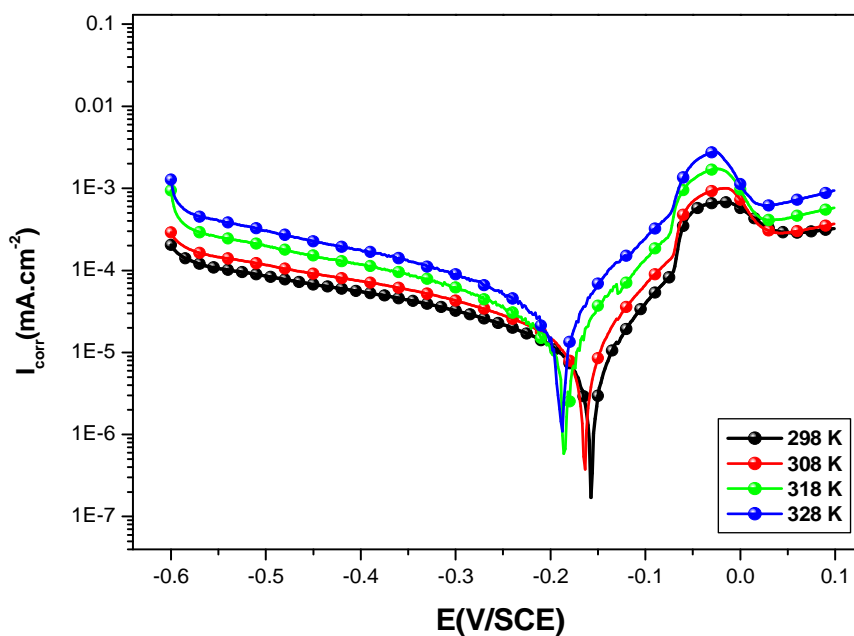
Fig 9 : Potentiodynamic polarization curves of Copper in 2M H₃PO₄ + 0.3M Nacl in the presence of 10⁻³ M of NPEPB.at different temperatures

3.6.Effect of temperature
3.6.1. Polarization curves
Temperature has a great effect on the corrosion phenomenon and the study of his effect on the corrosion rate and inhibition efficiency facilitates the calculation of kinetic and thermodynamic parameters for the inhibition and the

_____

adsorption processes. These parameters are useful in interpreting the type of adsorption by the inhibitor. It was shown from experimental and computational study that NPEPB molecule has the highest reactivity and inhibition efficiency and for this purpose, we will make potentiodynamic polarization in the range of temperature 298 to 328 K, in the absence and presence of NPEPB at 10^{-3} M. The corresponding data are shown in fig.8, 9 and Table 7.

Table 7: Effect of temperature on the copper corrosion in phosphoric acid containing chloride and at 10^{-3}M of NPEPB at different temperatures

Inhibitor	T°(K)	- E_{corr} (mV/SCE)	I_{corr} (µA/cm²)	- b_c (mV/dec)	E(%)
	298	118	149	322	-
	308	139	166	291	-
Blank	318	150	176	312	-
	328	170	186	309	-
	298	174	18	253	88
NPEPB	308	167	25	309	85
	318	186	35	306	80
	328	191	50	270	73

It is clear from fig.8 and table 7 that the increase of corrosion rate is more pronounced with the rise of temperature for blank solution. It has been observed from fig. 9 and table 7 that in the presence of NPEPB , I_{corr} is highly reduced. Also, the inhibition efficiencies decrease slightly with increasing of temperature indicating that higher temperature dissolution of copper predominates on adsorption of NPEPB at the metal surface and suggest a physical adsorption mode.

3.6.2. Kinetic parameters
In order to obtain more details on the corrosion process, activation kinetic parameters such as activation energies in free and inhibited acid were calculated using Arrhenius equation:
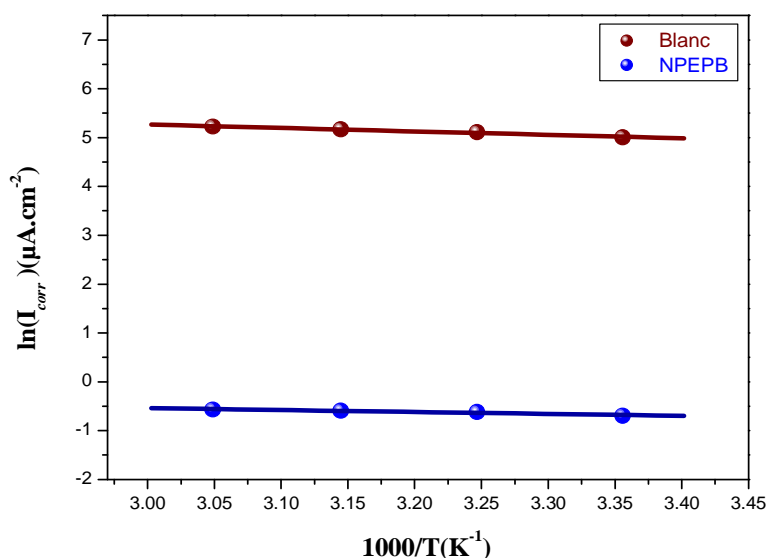
Fig 10: Arrhenius plots of Copper in 2M H_3PO_4 + 0.3M NaCl with and without 10^{-3}M of NPEPB

The activation parameters for the studied system (Ea, ΔH_a^* and ΔS_a^*) were estimated from the Arrhenius equation and transition state equation (Eq 15-16) :

$$I_{corr} = A \exp\left(\frac{-E_a}{RT}\right) \tag{15}$$

$$I_{corr} = \frac{RT}{Nh}\exp\left(\frac{\Delta S_a^*}{R}\right)\exp\left(-\frac{\Delta H_a^*}{RT}\right) \tag{16}$$

Where A is Arrhenius factor, E_a is the apparent activation corrosion energy, N is the Avogadro's number, h is the Plank's constant, and ΔH_a^* and ΔS_a^* are the enthalpy and the entropy changes of activation corrosion

_____

energies for the transition state complex. R is the perfect gas constant. The apparent activation energy was determined from the slopes of Ln (I_{corr}) vs $(1/T)$ graph depicted in Fig.10.
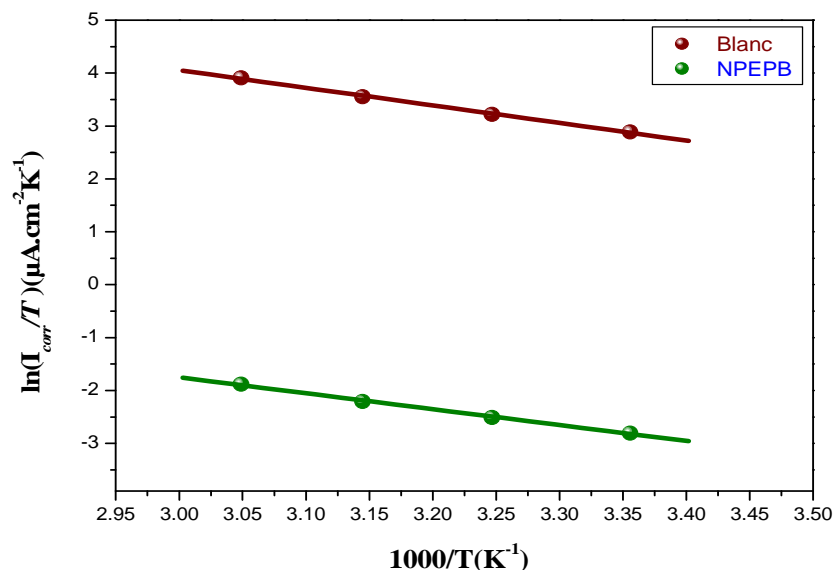
Fig 11. Relation between Ln (I_{corr}/T) and 1000/T at different temperatures

A plot of ln (I_{corr}/T) against 1/T (Fig. 11) gave a straight line with slope (ΔH_a^* /R) and intercept (ln(R/N A h) + (ΔS_a^* /R)), from which the values of ΔH_a^* and ΔS_a^* were calculated and listed in Table 8.

Table 8: Activation parameters for the corrosion of Copper in (2M H_3PO_4 + 0.3M NaCl) in the presence and absence of 10^{-3}M of NPEPB respectively

Inhibitor	E_a (kJ/mol)	ΔH_a (kJ/mol)	ΔS_a (J/mol)	E_a -ΔH_a (KJ/mol)	ΔG (kJ/mol) (T=298K)
Blank	5.90	3.31	-192.00	2,60	60.52
NPEPB	27.60	25.00	-137.01	2,60	65.83

The increase in activation energy (Ea) of inhibited solutions compared to the blank suggests that inhibitor is physically adsorbed on the corroding metal surface, while either unchanged or lower energy of activation in the presence of inhibitor suggest chemisorption [85]. As reported in Table8, Ea values increased greatly after the addition of the inhibitor. Hence corrosion inhibition of NPEPB is primarily occurring through physical adsorption.

The positive signs of ΔH_a^* reflected the endothermic nature of the Copper dissolution process. The value of ΔS_a^* is higher for the inhibited solution than that for the uninhibited solution. This phenomenon suggested that a decrease in randomness occurred on going from reactants to the activated complex. This might be the result of the adsorption of organic inhibitor molecule from the acidic solution which could be regarded as a quasi-substitution process between the organic compound in the aqueous phase and water molecules at electrode surface [86].

Large negative values of entropies show that the activated complex in the rate determining step is an association rather than dissociation step meaning that a decrease in disordering takes place on going from reactants to the activated complex [87-88].

3.7.Optical microscopy (OM)
In order to study the morphology of the carbon steel surfaces in contact with acidic solution, Optical microscopy OM was used. The Copper specimens after immersion in 2M H_3PO_4 + 0.3M NaCl solution for 7 days at 298K in the absence and presence of optimum concentration of NPEPB and CPEPB, the specimens were taken out, dried and kept in a dessicator. The OM images of Copper immersed in 2M H_3PO_4 + 0.3M in the absence and presence of the optimum concentration of the two inhibitors are shown in Fig.11

_____
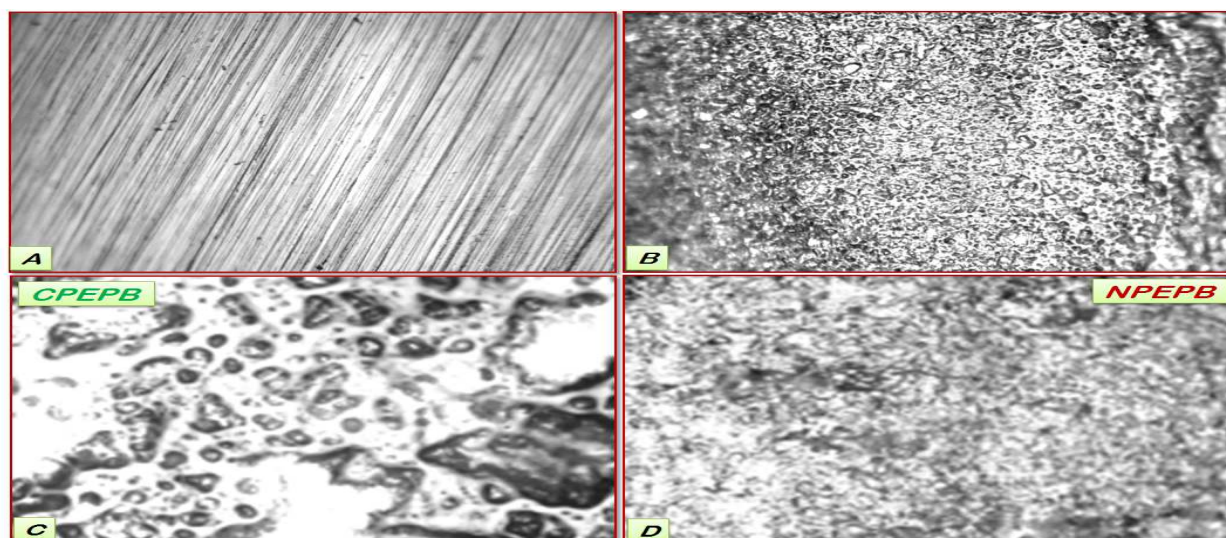
Fig. 11. OM (x200) of tinplate (A) before immersion (B) after 6h of immersion of copper in phosphoric acid (C and D) after 6h of immersion in 2M H₃PO₄+0.3M Nacl +10⁻³M of CPEPB and NPEPB at 298K

The resulting Optical microscopy micrographs reveal that, the surface was damaged owing to corrosion in absence of the inhibitor (blank), but in presence of the inhibitors, there is a much less damage on the surface. This is attributed to the formation of a good protective film on the copper surface.

CONCLUSION

From all the results, it can be concluded as follows:

• NPEPB and CPEPB ILs act as good Copper corrosion inhibitors in $2M\ H_3PO_4 + 0.3M$ Nacl. All electrochemical tests are in good agreement with the maximum percentage of inhibition efficiency obtained at the concentration of $10^{-3}\ M$.

• Potentiodynamic polarization measurements demonstrate that NPEPB and CPEPB act as mixed-type inhibitors.

• The adsorption of the two ILs molecules on the copper surface obeys The Langmuir adsorption isotherm. The negative values of free energy of adsorption (ΔG_{ads}) indicate that the adsorption process is spontaneous and chemically adsorbed on the copper surface and blocking the active sites.

• The results obtained from weight loss, polarization curves and EIS are in reasonably good agreement for NPEPB and CPEPB.

• Surface morphological studied with Optical microscopy micrographs showed that a film of inhibitors is formed on the copper electrode surface.

• Quantum chemical studies have been performed, using the B3LYP/6-31+G(d,p) method to investigate the properties of two newly synthesized ionic liquids and how their molecular properties relate to their ability to inhibit copper corrosion. A comparison of all the molecular properties suggests that NPEPB is a better corrosion inhibitor than CPEPB. This result agrees well with the experimental inhibition efficiencies reported in the study.

REFERENCES

[1]. Trabanelli G, *Corrosion* **1991**, 47, 410–419
[2]. Kim Ashassi-S H, Shaabani B, Seifzadeh D, *Appl Surf Sci*, **2005**, 239, 154–164.
[3]. Charles J., Catelin D., Dupoiron F., *Mater.Technol*. **1987,** 8, 309.
[4]. Sedrik A.J., *Corrosion* **1986**, 42, 376.
[5]. Nassif N., *Surf.Technol*. **1985**, 26, 189.
[6]. Trabanelli G., *Corrosion* **1991**, 47, 410.
[7]. M.H.Wahdan, A.A. Hermas, M.S. Morad, *Mater. Chem. Phys*. **2002**, 76, 111.
[8]. Bentiss F,Traisnel M,Lagrenee M, *Corros. Sci*. **2000**, 42, 127.
[9]. Li X,Tang L. Li, L, G. Mu, Liu G, *Corros. Sci*. **2006**, 48, 308.

_____

[10]. Benabdellah M, Aouniti A, Dafali A, Hammouti B, Benkaddour M, Yahyi A, Ettouhami A, *Appl. Surf. Sci.* **2006**, 252, 8341.

[11]. Emregül K.C, Hayvalı M, *Mater. Chem. Phys.* **2004**, 83, 209.

[12].Vivekananthan S S, Sakunthala P, Kesavan D, Gopiraman M, Alexramani V, Sulochana N, *Chem Sci Rev Lett* **2013**, 1(4), 195-200.

[13]. Raja P B, Sethuraman M G, *Mater Letter* **2008**, 62 (17–18), 2977-2979,

[14]. Belkhaouda M, Bammou L, Salghi R, Benali O, Zarrouk A, Zarrok H, Hammouti B, *J Mater Environ*, **2013**, 5(6), 1042-1051

[15]. Chinnaiyan T , Thavan K, *Chem Sci Rev Lett* **2014**, 3(9), 10-17.

[16]. Kesavan D, Parameswari K, Lavanya M, Beatrice V, Ayyannan G, Sulochana N, *Chem Sci Rev Lett* **2014**, 2(6),415-42.

[17]. Kim Ashassi-S H, Shaabani B, Seifzadeh D, *Appl Surf Sci*, **2005**, 239, 154–164.

[18]. Hua Z, Xia S.Q, Ma P.S, *Chem. Technol. Biotechnol*, **2005**, 80, 1089-1096.

[19]. Ibrahim M.A.M, Messali M, *Prod. Finish*. **2011**, 76, 14.

[20]. Sato T, Maruo T, Marukane S, Takagi K, *J. Power Sources*, **2004**,138, 253-261.

[21]. Endres F, *ChemPhysChem*, **2002**, 3, 144-154.

[22]. Ue M, Takeda M, Toriumi A, Kominato A, Hagiwara R, Ito Y, *J. Electrochem. Soc.,* **2003**, 150 A499-A502.

[23]. Ebenso E E, Alemu H, Umoren SA, Obot IB, *Int J Electrochem Sci* **2008**, 3, 1325.

[24]. Sami B A, *Int J Electrochem Sci* **2013**, 8, 10788 – 10804.

[25]. Sathianandhan B, Balahrishnan K, Subramnyan N, *Br Corros. J.* **1970**, 5, 270.

[26]. Tadros A B, Abdenaby B A, *J Electroanal Chem* **1988**, 246, 433.

[27]. Chin R J, Note K, *J Electrochem Sot* **1971**, 118, 545.

[28]. Eldakar N, Nobe K, *Corrosion* **1976**, 32, 238.

[29]. Eldakar N, Nobe K, *Corrosion* **1976**, 33, 128.

[30]. Agrawal R, Namboodhiri T K. G*, J Appl Electrochem* **1992**, 22, 383.

[31]. Abdenaby B A, Eltourhy A, Elgamal M, Mahgoub F, *Surf Coat Technol* **1986**, 27, 325.

[32]. Ateya B G, Elkhair A, Alqasimi R, *Corros Sci* **1982**, 22, 717.

[33]. Zucchi F, Trabanelli G, Brunoro G, *Corros Sci* **1992**, 33, 1135.

[34]. Zarrouk A, Messali M, Aouad M R, Assouag M, Zarrok H, Salghi R, Hammouti B, Chetouani A, *J Chem Pharm Res* **2012**, 4(7), 3427-3436.

[35]. Messali, M., *Arababian Journal of Chemistry*, **2014**, 7, (1), 63–70.

[36]. Endres F, *Chem. Phys. Chem.*, **2002**, 3, 144-154.

[37]. Sato T; Maruo T; Marukane S; Takagi K, J. *Power Source*., **2004**, 138, 253-261.

[38]. Ue M; Takeda M; Toriumi A; Kominato A; Hagiwara R; Ito Y, *J. Electrochem. Soc.*, **2003**, 150, 499-502.

[39]. Ngo, H. L; LeCompte, K.; Hargens, L; McEwen, A. B. *Thermochim. Acta* **2000**, 357-358 () 97-102.

[40]. Bonhôte, P.; Dias, A.-P.; Papageorgiou, N.; Kalyanasundaram, K.; Gratzel, M. *Inorg. Chem.* **1996**, 35, 1168-1178.

[41]. Dieter, K. M.; Dymek, C. J.; Heimer, N. E.; Rovang, J. W.; Wilkes, J. S. *J. Am. Chem. Soc.* **1988** ,110 () 2722-2726.

[42]. Forsyth, S.A., Pringle, J.M., MacFarlane, D.R. *Aust. J. Chem.* **2004**, 57,113.

[43]. Endres, F., El Abedin, S.Z., Matter, S., *Phys. Chem. Chem. Phys.* **2006**, 8, 2101.

[44]. Gasparac, R., Martin, C.R. Stupnisek-Lisac, *E. J. Electrochem. Soc.* **2000**, 147, 548.

[45]. Zhang, D.Q., Gao, L.X., Zhu, G.D. *Corros. Sci.* **2004**, 46, 3031.

[46]. Muralidharan, S., Iyer, S.V.K. *Anti-Corros. Met. Mater.* **1997**, 44,100.

[47]. Shi, S.C., Yi, P.G., Cao, C.Z., Wang, X.Y.J. *Chem. Ind. Eng. Chin.* **2005**,56,1112.

[48]. Zhang, Q.B., Hua, Y.X. *Electrochimica Acta* **2009**, 54, 1881–1887

[49]. Likhanova, N.V, Domínguez-Aguilar, M.A., Olivares-Xometl, O., Nava-Entzana, N., Arce, E., Dorantes, H. Corros , M.A.,Rafiquee, M.Z.A., Khan, S., Saxena, N. *J. Appl. Electrochem.* **2007**, 37, 1153.

[50]. Quraishi, M.A., Rafiquee, M.Z.A., Khan, S., Saxena, N. *J. Appl. Electrochem.* **2007**, 37, 1153.

[51]. Becke A. D. J., *Chem. Phys.*, **1992**, 96, 2155-2160.

[52]. Becke A. D. J, *Chem. Phys.*, **1993**, 98, 1372-1377.

[53]. Lee C., Yang W., Parr R. G., *Phys. Rev. B.*, **1988**,37,785-789.

[54]. Gaussian 03, Revision B.01, M.J. Frisch, et al., Gaussian, Inc., Pittsburgh, PA, **2003**.

[55]. Sangeetha M., Rajendran S., Sathiyabama J., Krishnaveni A., Shanthy P., Man-imaran N., Shyamaladevi B., Port. *Electrochim. Acta* **2011**, 29 (6), 429.

[56]. Rosliza R., Senin H.B., Wan Nik W.B., *Colloids Surf.* **2008**, 312,185.

[57]. Pinto G.M., Nayak J., Nityananda Shetty A., *Mater. Chem. Phys.* **2011**,125, 628.

[58]. Tsuru, T., Haruyama, S., Gijutsu, B., J. *Jpn. Soc. Corros. Eng.* **1978**, 27,573.

[59]. Aljourani J., Raeissi K., Golozar M.A., *Corros. Sci.* **2009**, 51,1836.

[60]. Ajmal M., Mideen A. S., Quraishi M. A., *Corros. Sci.* **1994**, 36,79.

_____

[61]. Hussin M.H., Kassim M.J.,. *Mater. Chem. Phys.* **2011**,125, 461.

[62]. Nasshorudin, D., **2010**. Master dissertation, Universiti Sains Malaysia, pp 20–30.

[63]. Sanat kumar B.S., Nayak J., Shetty A.N., *J. Coat. Technol. Res.* **2011**, 4, 1.

[64]. Avci G., *Colloids Surf. A.* **2008**, 317,730-736.

[65]. Solmaz R.; Kardas G.; M. çulha, B. Yazici, M. Erbil. *Electrochim. Acta.* **2008**, 53, 5941-5952.

[66]. Migahed M.A.; Nassar I.F.. *Electrochim. Acta.* **2008**, 53, 2877-2882.

[67]. Becke A.D., *J. Chem. Phys.* **1992**, 96, 9489.

[68]. Becke A.D., *J. Chem. Phys.* **1993**, 98, 1372.

[69]. Lee C., Yang W., Parr R.G., *Phys. Rev. B* **1988**, 37,785.

[70]. Gaussian 03, Revision B.01, Frisch M.J., et al., Gaussian, Inc., Pittsburgh, PA, **2003**.

[71]. Sastri V.S., Perumareddi J.R., *Corrosion* **1996**, 53, 671.

[72]. Pearson R.G., *Inorg. Chem.* **1988**, 27, 734.

[73]. Martinez S., *Mater. Chem. Phys.* **2002**, 77, 97.

[74]. Hassan H.H., *Electrochim. Acta* **2007**, 53, 1722.

[75]. Bockris J.O.M., Yang B., *J. Electrochem.* **1996**, 12, 853.

[76]. Hackerman N., Snavely Jr E.., Payne Jr J.S.., *J. Electrochem. Soc.* **1966**, 113, 677.

[77]. Lalitha A., Ramesh S., Rajeswari S., *Electrochim. Acta* **2005**, 51, 47.

[78]. Popova A., Christov M., Zwetanova A., *Corros. Sci.* **2007**,49, 2131.

[79]. Lukovits I., Ka´lma E., Zucchi N. F., *Corros.* **2001**, 57, 3.

[80]. Rodriguez L.M., Villamisr W., Martinez L., Daniel Glossman-Matnik, *Corros. Sci.* **2006**, 48, 4053.

[81]. Issa R.M., Awad M.K., Atlam F.M., *App. Surf. Sci.* **2008**, 255, 2433.

[82]. Li X., Deng S., Hui T., Li, *Electrochim. Acta* **2009**, 54, 4089.

[83]. Pearson R.G., *Inorg. Chem.* **1986**, 27, 734.

[84]. Koch E., Propellants, Explos., *Pyrotech.* **2005**, 30, 5.

[85]. Tsuru T., Haruyama S., Gijutsu B. J., *Soc. Corros. Eng.* **1978**, 27, 573.

[86]. Afia L., Salghi, R., Zarrouk, A., Zarrok, H., Benali, O., Hammouti,B., Al-Deyab, S.S., Chakir, A., Bazzi, L.,. Port. *Electrochim. Acta* **2012**, 30 (4), 267–279.

[87]. Oguzie E.E., *Corros. Sci.* **2007**, 49,1527. 35.

[88]. Martinez S., Stern I., *Appl. Surf. Sci.* **2002**, 199, 83.